Human Molecular Genetics, 2012, Vol. 21, No. 16 **3695–3702**
doi:10.1093/hmg/dds200
Advance Access published on May 31, 2012

Globozoospermia is mainly due to *DPY19L2* deletion via non-allelic homologous recombination involving two recombination hotspots

Elias Ellnati[1,†], Paul Kuentz[1,2,†], Claire Redin[1], Sara Jaber[1,3], Frauke Vanden Meerschaut[4], Joelle Makarian[1], Isabelle Koscinski[1,5], Mohammad H. Nasr-Esfahani[6], Aygul Demirol[7], Timur Gurgan[7], Noureddine Louanjli[8], Naeem Iqbal[9], Mazen Bisharah[9], Frédérique Carré Pigeon[10], H. Gourabi[11], Dominique De Briel[12], Florence Brugnon[13], Susan A. Gitlin[14], Jean-Marc Grillo[15], Kamran Ghaedi[6], Mohammad R. Deemeh[6], Somayeh Tanhaei[6], Parastoo Modarres[6], Björn Heindryckx[4], Moncef Benkhalifa[16], Dimitra Nikiforaki[4], Sergio C. Oehninger[14], Petra De Sutter[4], Jean Muller[1,17] and Stéphane Viville[1,18,*]

[1]Institut de Génétique et de Biologie Moléculaire et Cellulaire (IGBMC), Institut National de Santé et de Recherche Médicale (INSERM) U964, Centre National de Recherche Scientifique (CNRS) UMR1704, Université de Strasbourg, Illkirch 67404, France, [2]Centre Hospitalier Universitaire de Besançon, Besançon CEDEX 25030, France, [3]Institut Curie, 26 rue d'UIM, Paris Cedex 75248, France, [4]Department of Reproductive Medicine, University Hospital, De Pintelaan 185, Gent B-9000, Belgium, [5]Service de Biologie de la Reproduction, Centre Hospitalier Universitaire, Strasbourg 67000, France, [6]Department of Reproduction and Development, Reproductive Biomedicine Center, Royan Institute for Animal Biotechnology, ACECR, Isfahan, Iran, [7]Clinic Women Health, Infertility and IVF Center, Ankara, Turkey, [8]Laboratoire LABOMAC, Casablanca 20000, Morocco, [9]King Faisal Specialist Hospital and Research Center, Jeddah 21499, Kingdom of Saudi Arabia, [10]Service de Gynécologie-Obstétrique, CHU Reims, Institut mère-enfant Alix de Champagne, 45 rue Cognacq-Jay, Reims F-51092, France, [11]Royan Institute Reproductive Biomedicine and Stem Cell Research Center, Tehran, Iran, [12]Service de Microbiologie, Centre Hospitalier de Colmar, 39, avenue de la Liberté, Colmar 68024, France, [13]Laboratoire de Biologie de la Reproduction, Université Clermont 1, UFR Médecine, EA 975, Clermont Ferrand Cedex 1 F-63001, France, [14]Department of Obstetrics and Gynecology, The Jones Institute for Reproductive Medicine, Eastern Virginia Medical School, Norfolk, VA, USA, [15]Département d'Urologie, AP-HM, Salvatore Marseille, France, [16]ATL R&D Laboratory, 78320 la verrière et Unilabs, Paris 75116, France, [17]Laboratoire de Diagnostic Génétique, CHU Strasbourg, Nouvel Hôpital Civil, Strasbourg 67000, France and [18]Centre Hospitalier Universitaire, Strasbourg F-67000, France

Received March 28, 2012; Revised and Accepted May 22, 2012

To date, mutations in two genes, *SPATA16* and *DPY19L2*, have been identified as responsible for a severe teratozoospermia, namely globozoospermia. The two initial descriptions of the *DPY19L2* deletion lead to a very different rate of occurrence of this mutation among globospermic patients. In order to better estimate the contribution of *DPY19L2* in globozoospermia, we screened a larger cohort including 64 globozoospermic patients. Twenty of the new patients were homozygous for the *DPY19L2* deletion, and 7 were compound heterozygous for both this deletion and a point mutation. We also identified four additional mutated patients. The final mutation load in our cohort is 66.7% (36 out of 54). Out of 36 mutated patients, 69.4% are homozygous deleted, 19.4% heterozygous composite and 11.1% showed a homozygous point mutation. The mechanism underlying the deletion is a non-allelic homologous recombination (NAHR) between the flanking

*To whom correspondence should be addressed. Tel: +33 388653322; Fax: +33 388653201; Email: viville@igbmc.fr
†These authors contributed equally to this work.

low-copy repeats. Here, we characterized a total of nine breakpoints for the *DPY19L2* NAHR-driven deletion that clustered in two recombination hotspots, both containing direct repeat elements (*AluSq2* in hotspot 1, THE1B in hotspot 2). Globozoospermia can be considered as a new genomic disorder. This study confirms that *DPY19L2* is the major gene responsible for globozoospermia and enlarges the spectrum of possible mutations in the gene. This is a major finding and should contribute to the development of an efficient molecular diagnosis strategy for globozoospermia.

INTRODUCTION

Globozoospermia is a rare and severe teratozoospermia characterized by round-headed spermatozoa lacking an acrosome. The acrosome plays a crucial role during fertilization, allowing the spermatozoa to penetrate the zona pellucida and to reach the oocyte cytoplasmic membrane (1). Therefore, patients suffering from a complete form of globozoospermia are infertile. Round-headed spermatozoa do not present chromosomal abnormalities (2–4) and pregnancy can be obtained through ICSI, although at a low frequency (5–10). Previous analysis of globozoospermia families allowed us to identify mutations in two genes, *SPATA16* and *DPY19L2* (11,12). The deletion of exon 4 in *SPATA16* was found in an Ashkenazi Jewish family with three affected brothers. No other mutations were identified in a screen of 21 patients. A large deletion of ~200 kb encompassing the entire *DPY19L2* locus was detected in a consanguineous Jordanian family and in three additional unrelated patients (12). The gene, located on 12q14.2, has 22 exons encoding for a 9 transmembrane domain protein and is flanked by two low-copy repeats (LCRs) sharing 96.5% identity. The mechanism underlying the deletion is most probably a non-allelic homologous recombination (NAHR) between the flanking LCRs (13). Indeed, sequences with high nucleotide similarity (usually >95%) can serve as substrates for NAHR or ectopic recombination (14–16). Recently, a study of recurrent rearrangements associated with Smith–Magenis syndrome (SMS, MIM 182290) showed that NAHR crossover frequencies are correlated with the flanking LCR length and are inversely influenced by the distance between the LCRs (17). Homologous recombination on the Y chromosome is also known to impair fertility (18,19). However, so far, the deletion of *DPY19L2* is the first example where CNVs on autosomes are reported to be a causative infertility factor (20).

In our initial study, 19% of our patients (4 out of 21) were observed with such a deletion (12). In contrast, Harbuz *et al.* (21) detected a higher rate of *DPY19L2*-deleted patients (75%) in a cohort mainly composed of Tunisian patients. The difference is probably due to the broader geographic distribution of our patients (i.e. Algeria, France, Iran, Italy, Libya, Morocco and Tunisia).

In order to better estimate the contribution of *DPY19L2* in globozoospermia, we screened the largest cohort of globozoospermic patients to date, including 64 patients (from 13 different countries) and corresponding to 54 genetically independent individuals for all types of mutations. Twenty of the new patients were homozygous for the *DPY19L2* deletion, and seven were compound heterozygous for this deletion and a point mutation. We also identified four additional mutated patients. The final mutation load in our cohort is 66.7% (36 out of 54). Out of 36 mutated patients, 69.4% are homozygous deleted, 19.4% heterozygous composite and 11.1% showed a homozygous point mutation.

Recombination hotspots have been associated with genomic disorders and, when analyzing the sequence in the breakpoint (BP) cluster region, a common degenerate 13mer motif (CCNCCNTNNCCNC) was found (22), which has recently been elucidated as the *PRDM9* recognition binding motif (23–25). Here, we characterized nine new BPs for the *DPY19L2* NAHR-driven deletion defining two recombination hotspots, one containing the *PRDM9* recognition motif.

In this study, we confirmed that *DPY19L2* is the major gene responsible for globozoospermia, we enlarged the spectrum of possible mutations in the gene (deletion of the whole locus, nonsense, missense, splicing mutations and partial deletion) and we present globozoospermia as a new genomic disorder. This is a major finding and should contribute to the development of an efficient molecular diagnosis strategy for globozoospermia.

RESULTS

Deletion screening

In addition to our initial cohort of 21 patients, we recruited 33 new globozoospermic patients. As a first step, we screened for the deletion of *DPY19L2* in all 33 patients by performing a PCR of exon 10 and a PCR encompassing the previously described deletion BPs. Of these 33 new patients, 13 (Globo 29–31, 36, 39, 45, 48, 51, 54, 56, 57, 59, 61) did not show any amplification of exon 10, whereas the PCR of *DPY19L2* BPs revealed a fragment of 1700 bp, suggesting a homozygous deletion and a BP located within the 1700 bp fragment (Fig. 1A). Eight patients (Globo 28, 32, 33, 47, 50, 53, 58, 60) did not show any amplification at all, suggesting a homozygous deletion, but with a BP situated outside the tested region. We confirmed the deletion of most of the gene by testing for the presence of exons 4 and 16, which could not be amplified. Using specific oligonucleotides to walk on both sides of the deletion, we were able to amplify a common region of 1600 bp for two patients (Globo 28, 32). Sequencing of the 1600 bp fragment identified two BPs within an area of 117 bp (BP8 and BP9) (Fig. 2A). This second region of recombination is localized 9450 bp 3′ of the first one (Fig. 2B). For a third patient (Globo 33), we were able to amplify a fragment of 1500 bp. Sequencing of this fragment revealed another BP within a region of 265 bp (BP7) (Fig. 2A). This third region of recombination is situated 693 bp 3′ of the first one (Fig. 2B). For four patients (Globo

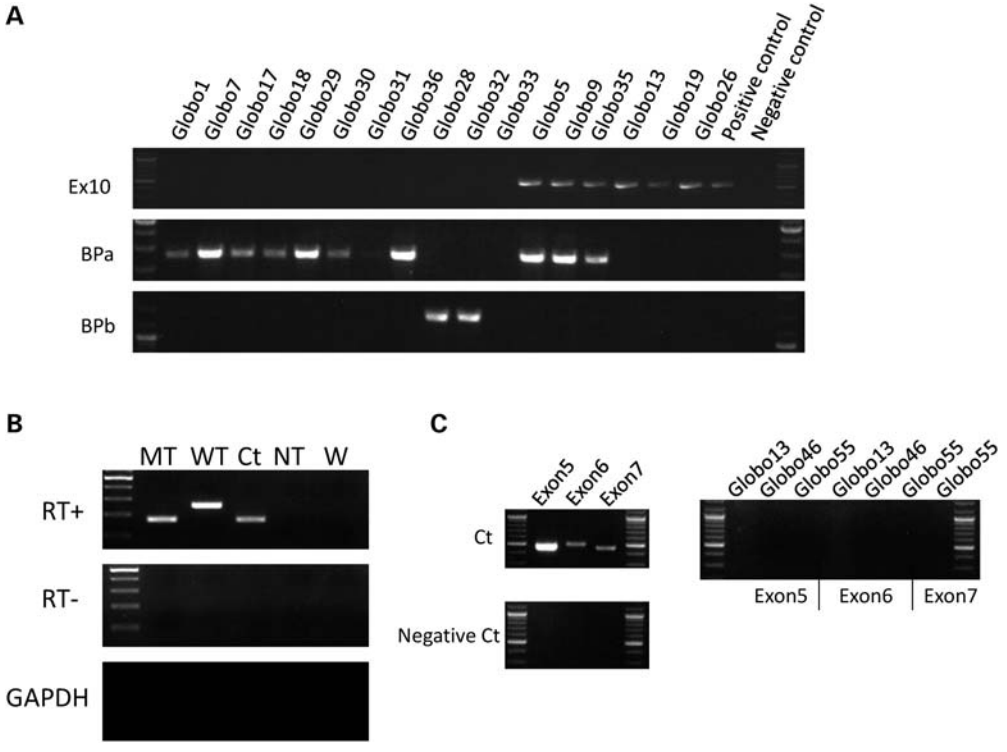

Figure 1. (**A**) PCR results of *DPY19L2* exon 10 and the BPs. Patients Globo1, Globo7, Globo17, Globo18, Globo29, Globo30, Globo31, Globo36, Globo28, Globo32, Globo33 are deleted for exon 10, whereas Gobo5, Gobo9, Gobo35, Gobo13, Gobo19, Gobo26 and the positive control showed an amplification of all of this exon. Globo1, Globo7, Globo17, Globo18, Globo29, Globo30, Globo31, Globo36, Globo28, Gobo5, Gobo9, Gobo35 showed an amplification for BP a, whereas Globo29 and Globo33 showed an amplification for BP b. For Globo39, 40, 42, 43, 45–48, 50, 51, 53, 54, 56–61, data are not shown. (**B**) Minigene constructs used to test the splicing of exon 11. Mt, mutant form of exon 11; WT, wild-type form of exon 11; Ct, construct without any cloned exon; NT, non-transfected cells; W, water. (**C**) PCR results for *DPY19L2* exons 5, 6 and 7. Globo13 and Globo46 are deleted for exons 5 and 6, whereas Globo55 is deleted for exons 5, 6 and 7. The positive control showed amplification of all these exons.

50, 53, 58, 60), we were not able to identify the BP. Five patients (Globo 35, 40, 42, 43, 46) showed an amplification of both exon 10 and the 1700 bp BP fragment, suggesting that these patients are heterozygous for the *DPY19L2* deletion (Fig. 1A). For the seven (Globo 34, 37, 38, 44, 49, 62, 63) remaining patients, exon 10 was detected, but no deletion could be found. Since we found one patient heterozygous for the deletion, we checked all remaining patients from our previous cohort. We identified two patients (Globo 5, 9) who were heterozygous for the *DPY19L2* deletion (Fig. 3A).

Point mutation screening

In a second step, in conjunction with screening for the *DPY19L2* deletion, we sequenced all coding exons and intron boundaries in the 7 compound heterozygous patients for the deletion and the 23 non-deleted patients (the exon localization of the mutations are shown in Fig. 2A). Concerning the heterozygous patients, sequence analysis of Globo5 revealed a variation in exon 8 (c.869G>A), leading to an amino acid change of a highly conserved residue (p.R290H) that was predicted to be deleterious by two programs: PolyPhen and SIFT (Supplementary Material, Table S1). Globo9 exhibited a variation in exon 9 (c.1033C>T), introducing a premature stop codon (p.Q345X). Globo35 presented a variation in exon 15 (c.1478C>G), leading to a non-synonymous mutation (p.T493R). This mutation is predicted to be deleterious by PolyPhen and tolerated by SIFT. Globo40 showed a variation in exon 21 (c.2038A>T), introducing a premature stop codon (p.K680X). Globo42 and 43, two unrelated patients, showed the same nucleotide deletion in exon 11 (c.1183delT), introducing a premature stop codon (p.S395LfsX7). Globo46 presented a deletion of exons 5 and 6. An aberrant splicing between exons 4 and 7 would give rise to a frame shift, introducing a premature stop codon (Supplementary Material, Table S1).

Among non-deleted patients, four, descending from consanguineous families, were found homozygous for a mutation. Globo26 showed a homozygous variation in exon 8 (c.892C>T), leading to a non-synonymous mutation (p.R298C), located at a strictly conserved amino acid position. This mutation is predicted to be deleterious by both PolyPhen and SIFT. Globo19 presented a homozygous donor splice-site mutation in intron 11 (c.1218+1G>A). Splice-site models (see Materials and Methods) predicted that the mutation disrupts the 5′ splice site of intron 11.

Unfortunately, the DPY19L2 protein presents a testis-restricted expression, and we were not allowed to use fresh sperm cells or to perform a testicular biopsy in these patients, in order to verify the predicted aberrant splicing *in vivo*. In order to test the prediction, minigene constructs were made, including either the wild-type (WT) or mutated form of exon 11

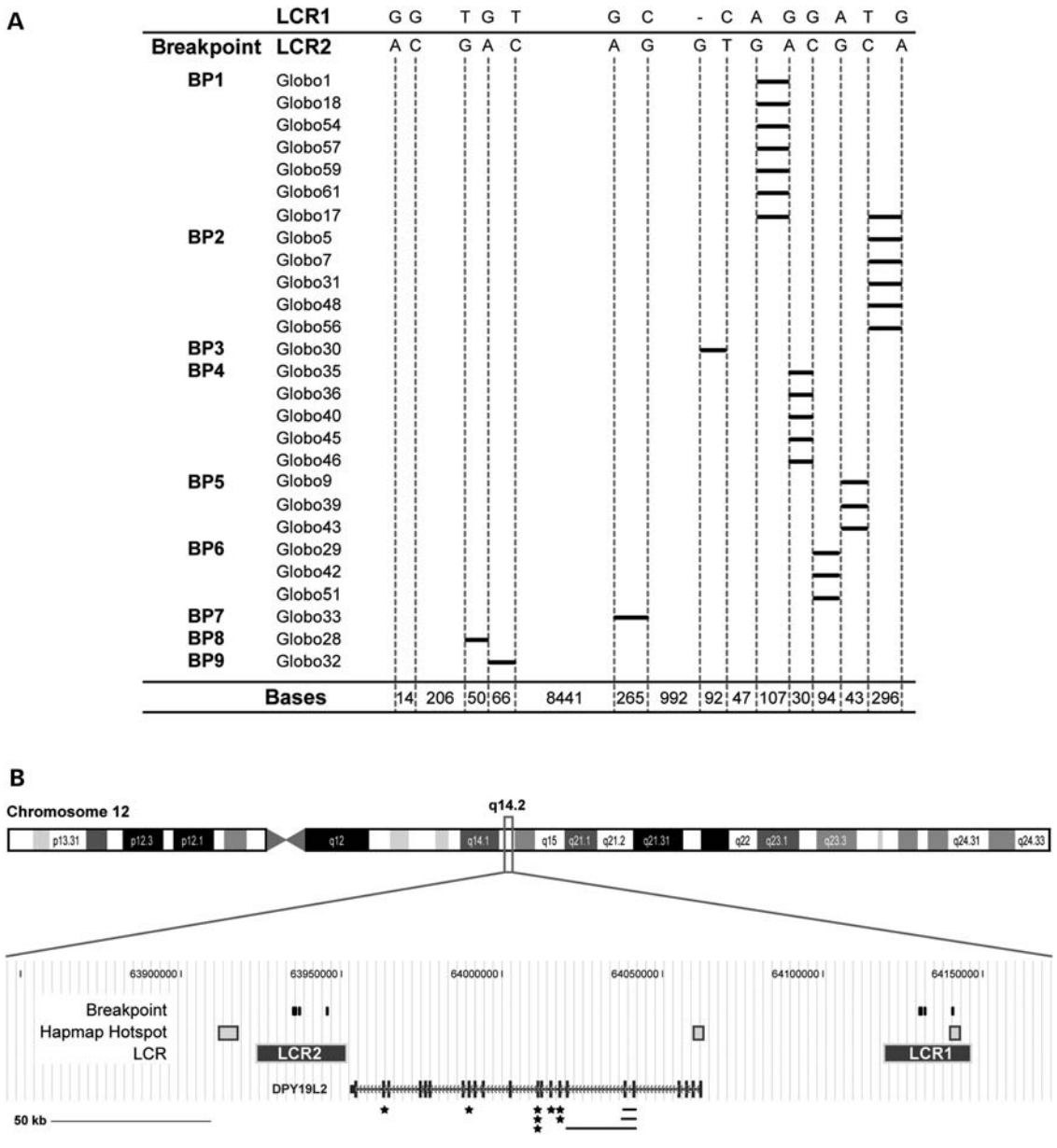

Figure 2. (**A**) For each LCR, the specific nucleotide differences within the hotspot regions are shown at the top. The length and distance between the different nucleotides are displayed at the bottom. The recombination region is represented for each patient by a black bar. The patients are ordered according to the nine BPs. (**B**) The *DPY19L2* locus is represented together with the two LCR, the HapMap recombination hotspots, the nine different BPs and the identified mutations (missenses are marked with a star and larger deletions are represented using a black horizontal line).

and flanking intronic sequences. These minigene constructs were transfected into COS1 and HeLa cells, and transcripts were analyzed by reverse transcription-PCR (RT-PCR) 48 h after the transfection. As shown in Figure 1B, WT exon 11 is invariably included in the final mRNA, as confirmed by the sequencing of the PCR product. In contrast, the mutated exon gives rise to one aberrant splicing form, leading to exon 11 skipping. An aberrant splicing of exon 11 could eventually give rise to a new splicing between exons 10 and 12 and would produce a protein with a deletion of 28 amino acids from position 378 to 406, corresponding to the seventh transmembrane helix (position 372–394).

We identified a homozygous deletion of exons 5 and 6 in Globo13. In order to pinpoint the two BP zones, subsequent amplifications on both sides of the exons were performed. Amplification across the deletion gave rise to a PCR fragment of 3500 bp for Globo13, whereas no amplification was possible from a control subject known to be fertile (Fig. 1C). Analysis of the sequence allowed the determination of the BPs and showed an insertion of 73 bp that corresponds to a part of a LINE sequence (Supplementary Material, Fig. S1). The deletion encompasses a 15.7 kb region with one BP located 8.35 kb from the 5′ side of exon 5 and the second one 4.36 kb from the 3′ side of exon 6. An aberrant splicing

A

Breakpoint zone	Point mutation	Patient	Origin
BP1	-	Globo1	Jordan
BP1	-	Globo18	France
BP1	-	Globo54	Iran
BP1	-	Globo57	Iran
BP1	-	Globo59	Iran
BP1	-	Globo61	Iran
BP2	p.R290H	Globo5	France
BP2	-	Globo7	Algeria
BP2	-	Globo31	Turkey
BP2	-	Globo48	Iran
BP2	-	Globo56	Iran
BP1/BP2	-	Globo17	France
BP3	-	Globo30	Saoudi Arabia
BP4	p.T493R	Globo35	Turkey
BP4	-	Globo36	Morocco
BP4	p.K680X	Globo40	Belgium
BP4	-	Globo45	Turkey
BP4	Ex5_6del	Globo46	USA
BP5	p.Q345X	Globo9	France
BP5	-	Globo39	Belgium
BP5	p.S395LfsX7	Globo43	Belgium
BP6	-	Globo29	Morocco
BP6	p.S395LfsX7	Globo42	Belgium
BP6	-	Globo51	Iran
BP7	-	Globo33	Turkey
BP8	-	Globo28	Morocco
BP9	-	Globo32	Turkey
-	Ex5_6del	Globo13	Iran
-	c.1218+1G>A	Globo19	Italy
-	p.R298C	Globo26	Morocco
-	Ex5_7del	Globo55	Iran
UBP	-	Globo47	Iran
UBP	-	Globo50	Iran
UBP	-	Globo53	Iran
UBP	-	Globo58	Iran
UBP	-	Globo60	Iran

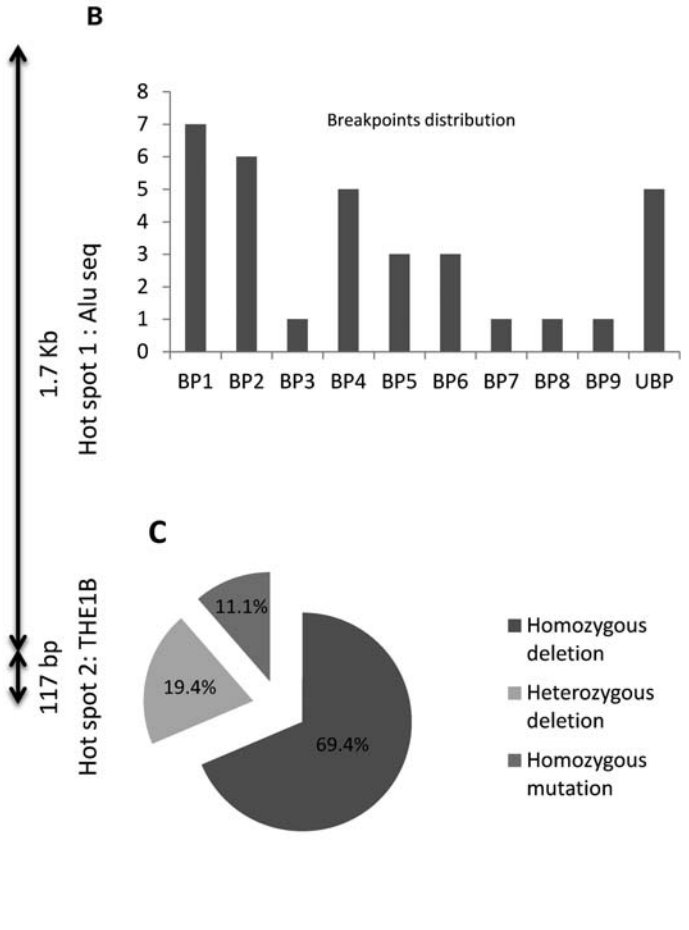

Figure 3. Distribution of BPs and mutations among patients. (**A**) The table presenting the type of BPs, mutations and patient origins. Vertical arrows delimit the two hotspots and their size. Hotspot 1 and hotspot 2 contain direct repeat elements, *Alu*Sq2 and THE1B, respectively. (**B**) The chart showing the distribution of the BPs among the patients totally deleted for *DPY19L2* (UBP, undetermined BP). (**C**) Pie chart showing the percentage of mutation types among the patients deleted and/or mutated for *DPY19L2*. Among these patients: 69.4% have a complete deletion of *DPY19L2* in the homozygous state; 19.4% have a complete deletion associated with a point mutation or a partial deletion; 11.1% have a point mutation or a partial deletion in the homozygous state.

between exons 4 and 7, if not degraded, would give rise to a frame shift, producing a truncated protein of 226 amino acids due to a premature stop codon at position 227. Since no repetitive sequence could be detected nearby, the deletion could be explained by a non-homologous end joining, which is often associated with the insertion of a DNA fragment at the BP (14). Globo46, who is compound heterozygous, also presented a deletion of exons 5 and 6, but with different BPs. Finally, Globo55 presented a deletion of exons 5, 6 and 7. An aberrant splicing between exons 4 and 8 would give rise to a protein with a deletion of 91 amino acids from position 196 to 287, corresponding to transmembrane domains 3, 4 and 5, at positions 195–215, 243–265 and 269–286, respectively (Supplementary Material, Table S1).

None of the variations described here were found, either in dbSNP v134 or when testing at least 188 control chromosomes.

BP analysis

We mapped linkage disequilibrium (LD) patterns and recombination rates in HapMap2 on chromosome 12. We observed that both LCR positions correlate with strongly suggested recombination spots, thus confirming the NAHR, which is the mechanism hypothesized to be responsible for the disease (26). Many other disorders involving NAHR between LCRs have been identified, such as DiGeorge syndrome/velocardiofacial syndrome, Williams–Beuren syndrome, Prader–Willi syndrome or Charcot–Marie–Tooth disease type 1A, which belong to the group of genomic disorders (27).

Previously, we identified two BPs (BP 1 and 2) localized close together in a region of 296 bp containing an *Alu* repetitive element (12). Sequence analysis of the amplification product across the deletions identified seven new BPs (BP3–9). Interestingly, seven of the BPs (BP1–7) are located in a small region of 1.7 kb, whereas the other two (BP8–9) are located in an area of 117 bp, 9.5 kb away from the first one (Fig. 2B). The underlying sequences of the BPs, as well as their genomic positions, are given in Supplementary Material, Figure S1. We can therefore suggest the presence of two recombination hotspots (hotspot 1 and 2, see Fig. 3A), comprising BP1–7 and BP8–9, respectively, both containing direct repeat elements (*Alu*Sq2 in hotspot 1, THE1B in hotspot 2). Interestingly, it was shown that AHR/NAHR hotspots

usually cluster within small regions of 1–2 kb of almost perfect identity, with repeat elements, transposons or minisatellites located nearby that act as substrates for double-strand breaks (22). Analysis of these hotspots in NAHR disorders identified a 13mer CCNCCNTNNCCNC motif frequently present in the flanking LCRs (22). We analyzed the sequences surrounding both identified recombination hotspots involved in the *DPY19L2* deletion and indeed found the PRDM9 13mer recognition motif (which is part of the THE1B repeat element), but only in hotspot 2 (Fig. 3A). Interestingly, hotspot 2 also coincides perfectly with a previously identified recombination hotspot (28) of chromosome 12 (Fig. 2B).

In total, we identified 32 patients with at least one deleted allele, among which BP1 occurs seven times, BP2 six times, BP4 five times, BP5 three times, BP6 three times and BP3, 7, 8, 9 were found only once (Fig. 3B). All recurrent BPs were found among patients originating from different regions, and patients from the same country showed different BPs (Fig. 3A). Out of 36 mutated patients, 69.4% were homozygous deleted, 19.4% heterozygous composite and 11.1% showed a homozygous point mutation (Fig. 3C).

DISCUSSION

The *DPY19L2* deletion was identified as being the major cause of globozoospermia in two different studies (12,21). It was shown by both groups that the most probable mechanism explaining this deletion is NAHR mediated by two LCRs surrounding *DPY19L2*. Thus, globozoospermia can be considered a new genomic disorder (27,29). Although both reports described a deletion rate of high frequency, a large difference was observed. Indeed, 19% (4 out of 21) of globozoospermic patients were found deleted in our study, whereas the other reported a frequency of 75% (15 out of 20). This difference could be due to a bias either in patient recruitment or in the limited number of patients analyzed. The higher frequency observed in Harbuz *et al*. (21) could be explained by the fact that most of the patients were Tunisians, whereas in our study, the patients were from seven different countries. Unfortunately, Harbuz *et al*. (21) were unable to localize the BPs, making it impossible to exclude a local founder effect in this cohort of globozoospermic patients. We present here the analysis of a larger cohort of globozoospermic patients, which allowed us, first, to refine the frequency rate of the deletion in our cohort, and, second, to enlarge the mutation spectrum. Indeed, in the context of this study and our previous work, we identified 24 homozygous deleted patients, 7 patients heterozygous for the deletion and presenting a point mutation in the remaining allele and 4 homozygous patients presenting a non-sense, a splicing mutation or deletions of exons 5 and 6 or exons 5 to 7 (Fig. 3A). In total, we identified nine BP zones, of which seven are clustered in a region of 1.7 kb and two in an area of 117 bp situated ~9 kb away from the first spot of recombination. Both regions seem to define two ectopic recombination hotspots for *DPY19L2* deletion (Supplementary Material, Fig. S1), each being <2 kb (in LCRs of ~27 kb) and containing a repeat element. Hotspot 1 accounts for almost all NAHR-driven *DPY19L2* deletions. In spite of its lower frequency, hotspot 2 contains the PRDM9 recognition binding motif, further supporting its involvement in the recombination mechanism (23,30). In addition, the fact that hotspot 2 coincides perfectly with a previously identified recombination hotspot supports the observation that NAHR and AHR share common features, including association with identical hotspot motifs.

We did not find any predominating BP. The fact that the same BPs are shared by patients from completely different regions and that patients from the same country can show different BPs tends to exclude any founder effect, even a recent one, and strongly suggests that the deletion results from recurrent events linked to the specific genomic architectural feature of this locus.

Our study allows us to calculate a more accurate prevalence of *DPY19L2* involvement in globozoospermia as a new genomic disorder. We analyzed a cohort of 54 globozoospermic patients and found that 36 of them were mutated for *DPY19L2* (66.7%). Despite the identification of subtle mutations, the most frequent alteration remains the deletion of the whole gene. Indeed, more than two-thirds (69%) of our patients are homozygously deleted, which also suggests that in one out of three of the cases, a search for point mutations is justified. We still have 18 patients with no identified mutation in *DPY19L2*, including 3 pairs of brothers, suggesting that new genes remain to be identified.

Since they do not present any other symptoms, globozoospermic patients are always recruited via *in vitro* fertilization centers. Considering the low frequencies of fertilization and birth obtained so far, one can wonder whether it is justified to propose that these couples go through the burden of such a heavy technology. A recent report, describing one globozoospermic patient, suggested that globozoospermia could be associated with the absence of phospholipase C zeta (PLCζ). This might explain the absence of fertilization, since PLCζ is the main physiological actor responsible for oocyte activation (31). An artificial activation, via a treatment with calcium ionophore, could improve fertilization rates and help to obtain embryos, thus increasing the chance of pregnancy (32). Such calcium ionophore activation treatment has been previously used successfully, considerably improving the fertilization and pregnancy rates in patients deficient for oocyte activation, including globozoospermic patients (33,34). It would be of great interest to see, in a larger cohort of globozoospermic patients, whether calcium ionophore activation would allow a better pregnancy rate and whether there is any correlation between the presence of a mutation in either *DPY19L2* or *SPATA16* and the pregnancy outcome. We are currently collecting DNA from globozoospermic patients for whom ICSI attempts have been done with or without oocyte activation.

MATERIALS AND METHODS

Patient recruitment and DNA preparation

Patients were selected by *in vitro* fertilization centers through a semen analysis implemented according to World Health Organization recommendations. Globozoospermia was diagnosed using a spermocytogram after a Harris–Shorr coloration.

Genomic DNA was extracted either from peripheral blood leukocytes using QIAamp DNA Blood Midi Kit (QIAGEN, Germany) or from saliva using Oragene DNA Self-Collection Kit (DNAgenotech, Ottawa, Canada), according to the manufacturer's instructions. This study was approved by the local Ethical Committee (Comité de protection de la personne, CPP) of Strasbourg University Hospital. For each case analyzed, informed written consent was obtained according to CPP recommendations.

PCR analysis

PCR covering all the exons of DPY19L2 and their exon–intron boundaries or the previously identified deletion (previously identified BPs BP1 and BP2) was performed using genomic DNA, and amplicons were sequenced by GATC (Konstanz, Germany). For the newly identified deletions, 5′ and 3′ walks were then carried out to identify the BPs. All primer sequences and PCR conditions are available in Supplementary Material, Table S2. Because of the high conservation level of duplicated regions, special care was taken to choose specific oligonucleotides with a unique sequence specifying a single location.

Plasmids and transfection

To study the effect of the c.1218+1G>A splice mutation, we constructed WT and mutated hybrid minigenes, using the pDUP33 vector (35). The genomic DNA region from Globo26 or from a control containing exon 11 (87 bp) and intronic flanking sequences (654 bp upstream from the 5′ exon end and 329 bp downstream from the 3′ exon end) were PCR-amplified using a forward primer (DPY19L2e11BamHI; 5′-GGGCCCtacatatggtattggtgatatcca-3′) and a reverse primer (DPY19L2e11BglII; 5′-AGATCTcactgcaatgagtacttaacc-3′). The 1063 bp PCR products were purified from agarose gel, using the Gel Band Purification Kit (Amersham Biosciences), and were sequentially digested by *Bam*HI and *Bgl*II. The insert was directionally cloned into the first intron of β-globin in the Dup33 plasmid. Recombinant plasmids were sequenced to confirm the presence of the mutated or the WT sequence. Transfection of plasmid DNA (WT, mutant and control pDUP33) in Cos and HeLa cells and RT-PCR were performed as previously described (11).

Bioinformatic analysis

Single-nucleotide variations (SNVs) were analyzed using the Alamut software (Interactive BioSoftware), which systematically gives access to several prediction algorithms. In particular, missense variations were tested with SIFT (36) and PolyPhen v2 (37). Missense and intronic variations were analyzed for splicing effects, using MaxEntScan (38), NNSPLICE (39) and HSF (40).

Allelic crossover hotspots [build 37 (36)], recombination rates from HapMap Phase II [build 36 (28)] and LD patterns from the 1000 Genomes project [build 37 (41)] were mapped onto the *DPY19L2* locus using the UCSC browser (42).

SUPPLEMENTARY MATERIAL

Supplementary Material is available at *HMG* online.

ACKNOWLEDGEMENTS

We are very grateful to James R Lupski, Claudia Carvalho and our colleagues Jean-Louis Mandel and Julie Thompson for their critical reading of this manuscript. We are also grateful for the services of the Institute of Genetics and Molecular and Cellular Biology (IGBMC).

Conflict of Interest statement. None declared.

AUTHORS' ROLES

Contributors E.E., P.K. and S.V. designed the study; E.E., P.K., S.J., J.M. and I.K. performed genetic analysis and mutation screening; F.V.M., M.H.N.-E., A.D., T.G., N.L., N.I., M.B., F.C.P., H.G., D.D., F.B., S.A.G., J.-M.G., S.C.O., P.D. recruited patients and collected clinical data; C.R. and J.M. contributed to the bioinformatics analysis; E.E., P.K., C.R., J.M. and S.V. contributed to analysis and interpretation of data; E.E., C.R., J.M. and S.V. wrote the manuscript.

FUNDING

This work was supported by the French Centre National de la Recherche Scientifique (CNRS), Institut National de la Santé et de la Recherche Médicale (INSERM), the Ministère de l'Education Nationale, the Enseignement Supérieur et de la Recherche, the University of Strasbourg, the University Hospital of Strasbourg and the Agence de la BioMédecine.

REFERENCES

1. Ikawa, M., Inoue, N., Benham, A.M. and Okabe, M. (2010) Fertilization: a sperm's journey to and interaction with the oocyte. *J. Clin. Invest.*, **120**, 984–994.
2. Carrell, D.T., Emery, B.R. and Liu, L. (1999) Characterization of aneuploidy rates, protamine levels, ultrastructure, and functional ability of round-headed sperm from two siblings and implications for intracytoplasmic sperm injection. *Fertil. Steril.*, **71**, 511–516.
3. Machev, N., Gosset, P. and Viville, S. (2005) Chromosome abnormalities in sperm from infertile men with normal somatic karyotypes: teratozoospermia. *Cytogenet. Genome Res.*, **111**, 352–357.
4. Viville, S., Mollard, R., Bach, M.L., Falquet, C., Gerlinger, P. and Warter, S. (2000) Do morphological anomalies reflect chromosomal aneuploidies? Case report. *Hum. Reprod.*, **15**, 2563–2566.
5. Banker, M.R., Patel, P.M., Joshi, B.V., Shah, P.B. and Goyal, R. (2009) Successful pregnancies and a live birth after intracytoplasmic sperm injection in globozoospermia. *J. Hum. Reprod. Sci.*, **2**, 81–82.
6. Bechoua, S., Chiron, A., Delcleve-Paulhac, S., Sagot, P. and Jimenez, C. (2009) Fertilisation and pregnancy outcome after ICSI in globozoospermic patients without assisted oocyte activation. *Andrologia*, **41**, 55–58.
7. Coetzee, K., Windt, M.L., Menkveld, R., Kruger, T.F. and Kitshoff, M. (2001) An intracytoplasmic sperm injection pregnancy with a globozoospermic male. *J. Assist. Reprod. Genet.*, **18**, 311–313.
8. Dirican, E.K., Isik, A., Vicdan, K., Sozen, E. and Suludere, Z. (2008) Clinical pregnancies and livebirths achieved by intracytoplasmic injection of round headed acrosomeless spermatozoa with and without oocyte activation in familial globozoospermia: case report. *Asian J. Androl.*, **10**, 332–336.

9. Kilani, Z., Ismail, R., Ghunaim, S., Mohamed, H., Hughes, D., Brewis, I. and Barratt, C.L. (2004) Evaluation and treatment of familial globozoospermia in five brothers. *Fertil. Steril.*, **82**, 1436–1439.
10. Sermondade, N., Hafhouf, E., Dupont, C., Bechoua, S., Palacios, C., Eustache, F., Poncelet, C., Benzacken, B., Levy, R. and Sifer, C. (2011) Successful childbirth after intracytoplasmic morphologically selected sperm injection without assisted oocyte activation in a patient with globozoospermia. *Hum. Reprod.*, **26**, 2944–2949.
11. Dam, A.H., Koscinski, I., Kremer, J.A., Moutou, C., Jaeger, A.S., Oudakker, A.R., Tournaye, H., Charlet, N., Lagier-Tourenne, C., van Bokhoven, H. *et al.* (2007) Homozygous mutation in SPATA16 is associated with male infertility in human globozoospermia. *Am. J. Hum. Genet.*, **81**, 813–820.
12. Koscinski, I., Elinati, E., Fossard, C., Redin, C., Muller, J., Velez de la Calle, J., Schmitt, F., Ben Khelifa, M., Ray, P.F., Kilani, Z. *et al.* (2011) DPY19L2 deletion as a major cause of globozoospermia. *Am. J. Hum. Genet.*, **88**, 344–350.
13. Stankiewicz, P. and Lupski, J.R. (2002) Genome architecture, rearrangements and genomic disorders. *Trends Genet.*, **18**, 74–82.
14. Gu, W., Zhang, F. and Lupski, J.R. (2008) Mechanisms for human genomic rearrangements. *Pathogenetics*, **1**, 4.
15. Inoue, K. and Lupski, J.R. (2002) Molecular mechanisms for genomic disorders. *Annu. Rev. Genomics Hum. Genet.*, **3**, 199–242.
16. Lupski, J.R. (2004) Hotspots of homologous recombination in the human genome: not all homologous sequences are equal. *Genome Biol.*, **5**, 242.
17. Liu, P., Lacaria, M., Zhang, F., Withers, M., Hastings, P.J. and Lupski, J.R. (2011) Frequency of nonallelic homologous recombination is correlated with length of homology: evidence that ectopic synapsis precedes ectopic crossing-over. *Am. J. Hum. Genet.*, **89**, 580–588.
18. Blanco, P., Shlumukova, M., Sargent, C.A., Jobling, M.A., Affara, N. and Hurles, M.E. (2000) Divergent outcomes of intrachromosomal recombination on the human Y chromosome: male infertility and recurrent polymorphism. *J. Med. Genet.*, **37**, 752–758.
19. McLachlan, R.I. and O'Bryan, M.K. (2010) Clinical review: state of the art for genetic testing of infertile men. *J. Clin. Endocrinol. Metab.*, **95**, 1013–1024.
20. Carvalho, C.M., Zhang, F. and Lupski, J.R. (2011) Structural variation of the human genome: mechanisms, assays, and role in male infertility. *Syst. Biol. Reprod. Med.*, **57**, 3–16.
21. Harbuz, R., Zouari, R., Pierre, V., Ben Khelifa, M., Kharouf, M., Coutton, C., Merdassi, G., Abada, F., Escoffier, J., Nikas, Y. *et al.* (2011) A recurrent deletion of DPY19L2 causes infertility in man by blocking sperm head elongation and acrosome formation. *Am. J. Hum. Genet.*, **88**, 351–361.
22. Myers, S., Freeman, C., Auton, A., Donnelly, P. and McVean, G. (2008) A common sequence motif associated with recombination hot spots and genome instability in humans. *Nat. Genet.*, **40**, 1124–1129.
23. Baudat, F., Buard, J., Grey, C., Fledel-Alon, A., Ober, C., Przeworski, M., Coop, G. and de Massy, B. (2011) PRDM9 is a major determinant of meiotic recombination hotspots in humans and mice. *Science*, **327**, 836–840.
24. McVean, G. and Myers, S. (2010) PRDM9 marks the spot. *Nat. Genet.*, **42**, 821–822.
25. Myers, S., Bowden, R., Tumian, A., Bontrop, R.E., Freeman, C., MacFie, T.S., McVean, G. and Donnelly, P. (2010) Drive against hotspot motifs in primates implicates the PRDM9 gene in meiotic recombination. *Science*, **327**, 876–879.
26. Lindsay, S.J., Khajavi, M., Lupski, J.R. and Hurles, M.E. (2006) A chromosomal rearrangement hotspot can be identified from population genetic variation and is coincident with a hotspot for allelic recombination. *Am. J. Hum. Genet.*, **79**, 890–902.
27. Lupski, J.R. (2009) Genomic disorders ten years on. *Genome Med.*, **1**, 42.
28. International HapMap Consortium (2003) The International HapMap Project. *Nature*, **426**, 789–796.
29. Lupski, J.R. (1998) Genomic disorders: structural features of the genome can lead to DNA rearrangements and human disease traits. *Trends Genet.*, **14**, 417–422.
30. Berg, I.L., Neumann, R., Lam, K.W., Sarbajna, S., Odenthal-Hesse, L., May, C.A. and Jeffreys, A.J. (2011) PRDM9 variation strongly influences recombination hot-spot activity and meiotic instability in humans. *Nat. Genet.*, **42**, 859–863.
31. Kashir, J., Heindryckx, B., Jones, C., De Sutter, P., Parrington, J. and Coward, K. (2010) Oocyte activation, phospholipase C zeta and human infertility. *Hum. Reprod. Update*, **16**, 690–703.
32. Taylor, S.L., Yoon, S.Y., Morshedi, M.S., Lacey, D.R., Jellerette, T., Fissore, R.A. and Oehninger, S. (2010) Complete globozoospermia associated with PLCzeta deficiency treated with calcium ionophore and ICSI results in pregnancy. *Reprod. Biomed. Online*, **20**, 559–564.
33. Heindryckx, B., De Gheselle, S., Gerris, J., Dhont, M. and De Sutter, P. (2008) Efficiency of assisted oocyte activation as a solution for failed intracytoplasmic sperm injection. *Reprod. Biomed. Online*, **17**, 662–668.
34. Heindryckx, B., Van der Elst, J., De Sutter, P. and Dhont, M. (2005) Treatment option for sperm- or oocyte-related fertilization failure: assisted oocyte activation following diagnostic heterologous ICSI. *Hum. Reprod.*, **20**, 2237–2241.
35. Dominski, Z. and Kole, R. (1992) Cooperation of pre-mRNA sequence elements in splice site selection. *Mol. Cell. Biol.*, **12**, 2108–2114.
36. Kumar, P., Henikoff, S. and Ng, P.C. (2009) Predicting the effects of coding non-synonymous variants on protein function using the SIFT algorithm. *Nat. Protoc.*, **4**, 1073–1081.
37. Adzhubei, I.A., Schmidt, S., Peshkin, L., Ramensky, V.E., Gerasimova, A., Bork, P., Kondrashov, A.S. and Sunyaev, S.R. (2010) A method and server for predicting damaging missense mutations. *Nat. Methods*, **7**, 248–249.
38. Yeo, G. and Burge, C.B. (2004) Maximum entropy modeling of short sequence motifs with applications to RNA splicing signals. *J. Comput. Biol.*, **11**, 377–394.
39. Reese, M.G., Eeckman, F.H., Kulp, D. and Haussler, D. (1997) Improved splice site detection in Genie. *J. Comput. Biol.*, **4**, 311–323.
40. Desmet, F.O., Hamroun, D., Lalande, M., Collod-Beroud, G., Claustres, M. and Beroud, C. (2009) Human Splicing Finder: an online bioinformatics tool to predict splicing signals. *Nucleic Acids Res.*, **37**, e67.
41. 1000 Genomes Project Consortium (2010) A map of human genome variation from population-scale sequencing. *Nature*, **467**, 1061–1073.
42. Karolchik, D., Hinrichs, A.S. and Kent, W.J. (2011) The UCSC Genome Browser. *Curr. Protoc. Hum. Genet.*, **18**, 18.6.1–18.6.33.